

Stability of laser cavity-solitons for metrological applications F

Cite as: Appl. Phys. Lett. **122**, 121104 (2023); <https://doi.org/10.1063/5.0134147>

Submitted: 08 November 2022 • Accepted: 03 February 2023 • Published Online: 20 March 2023

Published open access through an agreement with JISC Collections

 A. Cutrona,  M. Rowley,  A. Bendahmane, et al.

COLLECTIONS

F This paper was selected as Featured



View Online



Export Citation



CrossMark

ARTICLES YOU MAY BE INTERESTED IN

[Electrode pattern definition in ultrasound power transfer systems](#)

Applied Physics Letters **122**, 124101 (2023); <https://doi.org/10.1063/5.0139866>

[Magnetoplasmonics in confined geometries: Current challenges and future opportunities](#)

Applied Physics Letters **122**, 120502 (2023); <https://doi.org/10.1063/5.0136941>

[Thin-film lithium niobate electro-optic modulators: To etch or not to etch](#)

Applied Physics Letters **122**, 120501 (2023); <https://doi.org/10.1063/5.0142232>



Time to get excited.
Lock-in Amplifiers – from DC to 8.5 GHz

[Find out more](#)

 Zurich Instruments

Stability of laser cavity-solitons for metrological applications

Cite as: Appl. Phys. Lett. **122**, 121104 (2023); doi: [10.1063/5.0134147](https://doi.org/10.1063/5.0134147)

Submitted: 8 November 2022 · Accepted: 3 February 2023 ·

Published Online: 20 March 2023










View Online



Export Citation



CrossMark

A. Cutrona,^{1,2,a)}  M. Rowley,²  A. Bendahmane,²  V. Cecconi,^{1,2}  L. Peters,^{1,2}  L. Olivieri,^{1,2} 
B. E. Little,³  S. T. Chu,⁴  S. Stivala,⁵  R. Morandotti,⁶  D. J. Moss,⁷  J. S. Toterogongora,^{1,2} 
M. Peccianti,^{1,2}  and A. Pasquazi^{1,2,a)} 

AFFILIATIONS

¹Emergent Photonics Research Centre, Department of Physics, Loughborough University, Loughborough LE11 3TU, United Kingdom

²Emergent Photonics Lab (Epic), Department of Physics and Astronomy, University of Sussex, Brighton BN1 9QH, United Kingdom

³QXP Technology Inc., Xi'an, China

⁴Department of Physics, City University of Hong Kong, Tat Chee Avenue, Hong Kong, China

⁵Department of Engineering, University of Palermo, Viale delle Scienze, Building 9, Palermo 90128, Italy

⁶INRS-EMT, 1650 Boulevard Lionel-Boulet, Varennes, Québec J3X 1S2, Canada

⁷Optical Sciences Centre, Swinburne University of Technology, Hawthorn, VIC 3122, Australia

^{a)} Authors to whom correspondence should be addressed: a.cutrona@lboro.ac.uk and a.pasquazi@lboro.ac.uk

ABSTRACT

Laser cavity-solitons can appear in systems comprised of a nonlinear microcavity nested within an amplifying fiber loop. These states are robust and self-emergent and constitute an attractive class of solitons that are highly suitable for microcomb generation. Here, we present a detailed study of the free-running stability properties of the carrier frequency and repetition rate of single solitons, which are the most suitable states for developing robust ultrafast and high repetition rate comb sources. We achieve free-running fractional stability on both optical carrier and repetition rate (i.e., 48.9 GHz) frequencies on the order of 10^{-9} for a 1 s gate time. The repetition rate results compare well with the performance of state-of-the-art (externally driven) microcomb sources, and the carrier frequency stability is in the range of performance typical of modern free-running fiber lasers. Finally, we show that these quantities can be controlled by modulating the laser pump current and the cavity length, providing a path for active locking and long-term stabilization.

© 2023 Author(s). All article content, except where otherwise noted, is licensed under a Creative Commons Attribution (CC BY) license (<http://creativecommons.org/licenses/by/4.0/>). <https://doi.org/10.1063/5.0134147>

Cavity-solitons^{1,2} are an important class of dissipative solitary waves studied in both spatial and temporal configurations. In the field of “Microcombs” or optical frequency combs achieved in nonlinear microcavities,^{3,4} temporal cavity-solitons^{5,6} have been instrumental in harnessing phase coherence, eventually enabling many practical applications.^{7–16} Among the different properties of a pulsed source, the long-term stability of the two defining quantities of the spectrum,¹⁷ i.e., the carrier (or the carrier-envelope offset) and the repetition rate frequencies, defines the metrological quality of the comb laser.

To date, the most investigated microcomb states are the cavity-soliton solutions obtained in continuous-wave driven microresonators, which can be well-described by the Lugiato–Lefever equation.^{18,19} Such structures originate from a four-wave mixing process, which transfers the energy from a coherent “driving” laser (pump) to the

comb lines. Early investigations on the stability properties of electro-optic modulated combs²⁰ reported a fractional stability of the repetition rate of 2×10^{-8} at 1 s gate time and have motivated further studies. Soliton states, in particular, later demonstrated similar figures—typical free-running repetition rate fractional stability at 1 s gate time on the order of 10^{-9} [e.g., 7×10^{-8} ,²¹ 6.6×10^{-8} ,²² 4.5×10^{-9} ,²³ and 2×10^{-9} (Ref. 24)]. The engineering of thermal effects^{25–28} has been shown to benefit soliton robustness. In Ref. 27, the authors reached free-running fractional stability of approximately 1×10^{-9} for single soliton operation, relying on a Brillouin laser pumping scheme to exploit thermo-optical self-stabilization,²⁹ although Allan deviations were not reported. These excellent free-running properties allowed the implementation of active locking schemes,^{23,24,27} and microcombs demonstrated several breakthroughs as metrological references.^{12,15,28,30–39}

Among the different techniques for microcomb generation, we introduced a microresonator-filtered laser approach^{40,41} that can sustain the laser cavity-solitons.^{42–45} These pulses arise when light is allowed to resonate within two group-velocity matched nested cavities, namely a nonlinear micro-ring and an amplifying cavity. One of the distinctive traits of this topology is the absence of any external coherent driving source, in contrast to most microcombs, or of an ultrafast saturable absorber, in contrast to most passive mode-locking lasers. A very effective implementation utilizes an erbium-doped fiber as the amplifying element.^{42–45} The filtering action of the microresonator constrains the repetition rate of such a system to be an integer multiple of the main cavity free-spectral range (FSR). It selects only the main cavity modes falling inside the microresonator resonances in coherent operation. To this aim, the fiber cavity needs to have an FSR comparable to or smaller than the linewidth of the microcavity resonances. As such, this scheme practically allows operating a fiber laser at an extremely high harmonic of the cavity round trip frequency. In our experiments, in particular, a typical single soliton implementation operates between the 500th and the 700th harmonic of the fiber cavity FSR (usually between 70 and 100 MHz) when using a 50 GHz microresonator. Harmonic mode locking (HML) techniques have been largely investigated in pulsed fiber lasers.^{46–51} However, depending on the HML regime, the laser cavity may fill with many pulses whose relative distance can generally fluctuate. Supermode instabilities typically affect HML fiber lasers,^{52,53} which usually do not achieve the performances of metrological, passive-mode-locked fiber lasers operating at the cavity FSR. The frequency of an individual comb line of state-of-the-art metrological fiber lasers can show fractional stability well below 10^{-10} at 1 s of gate time in a free-running configuration, e.g., 5×10^{-10} in Ref. 54 and 1×10^{-11} in Ref. 55. These facts motivate further investigations of the stability properties of a microresonator-filtered fiber laser. Finally, recent approaches based on driven loop configurations^{56–60} are becoming increasingly popular, motivating the need to understand multi-cavity sources further.

Our system can be configured to indefinitely maintain soliton states, which are its dominant attractors⁴⁴ and are spontaneously initiated and preserved by the balance of the slow nonlinearities driving the system. The nonlinear locking properties enhance the soliton state's robustness and stability against external perturbations. However, an important open question is how the robustness of the soliton is effectively translated into its frequency stability properties.

In this work, we perform a detailed study of the long-term stability of the comb carrier and repetition rate frequencies. We start with a characterization in free-running operation, focusing on the Allan deviations for averaging times > 1 ms. We show how these frequencies can be controlled by manipulating easily accessible experimental parameters, such as the amplifying cavity length and the pump current. The free-running Allan deviations at 1 s gate time are 3.55×10^{-10} and 4.95×10^{-9} for the carrier and repetition rate frequencies, respectively.

Our comb scheme relies on a nested-cavity design [Fig. 1(a)]. A four-port nonlinear Kerr microresonator (FSR = 48.89 GHz) is nested into a polarization-maintaining amplifying fiber loop (main cavity). The main cavity comprises a free-space delay line, polarization controllers, and a bandpass filter (BPF) to provide a smooth shape to the gain amplification spectrum.

Coherent pulsed sources can be described by two main degrees of freedom: the carrier frequency (f_c) and the repetition rate frequency

(f_{rep}). We characterized the stability of both quantities with the setup depicted in Fig. 1(b). In our measurements, the microcomb signal interfered with a comb (Menlo Systems) tied to a GPS (Global Positioning System) reference signal, and a dense wavelength division multiplexing (DWDM) filter selected the portion of the spectrum relative to the carrier frequency $f_c \approx 194.2$ THz (corresponding to $\lambda_c \approx 1543.7$ nm). The signal generated by beating with the reference comb line was then detected and electrically filtered [see Fig. 1(c)].

We also synchronously acquired the repetition rate frequency $f_{rep} \approx 48.894$ GHz. To this aim,⁶¹ we modulated a portion of the through output port signal driving an electro-optic modulator (EOM) in saturation with a GPS-referenced microwave oscillator (Keysight EXG N5173B). The GPS-referenced microwave oscillator drove the EOM at a frequency $f_0 \approx 8.146$ GHz. In this way, we obtained a rich harmonic content of the modulating signal resulting in multiple sidebands around each comb line. With our choice of values, the frequency difference between the third sidebands of any adjacent comb line was about 20 MHz, resulting in an RF beat-note signal, which we extracted and frequency-counted [Figs. 1(b) and 1(c)]. We refer to the frequency of this beat-note with f_b . Within this scheme, given the modulation frequency f_0 , the repetition rate is

$$f_{rep} = f_b + 6f_0. \quad (1)$$

We measured f_{rep} and the variations of f_c with two synchronized frequency counters. The reference comb, microwave oscillator, and frequency counters were locked to the same GPS-referenced signal. We verified that the oscillator did not affect our stability measurements for gate times greater than 1 ms.

When set in stable single soliton operation, the system provided a 48.894 GHz repetition rate comb with a 60 nm bandwidth, which could be collected at the two output ports of the system, as highlighted in Fig. 1(a). These states were further monitored with an optical spectrum analyzer (OSA) and an auto-correlator (AC).

The spectra at the Through and Drop ports of the microcavity of a typical single soliton are reported in Figs. 1(d) and 1(e), respectively, together with the gain spectrum of the system (in yellow), which has a much smaller bandwidth than the generated comb. A typical auto-correlation trace is reported in Fig. 1(f) over a window of 80 ps, showing the presence of four background-free pulses, as expected for a ~ 50 GHz train of pulses. An electrical spectrum analyzer (ESA) trace of the down-converted repetition rate signal is also shown in Fig. 1(g).

A typical long-term characterization of a free-running single soliton state is reported in Fig. 2. We acquired the frequency stability signals for a 15-min-long segment of stable soliton operation, along with AC traces [Fig. 2(a)] and OSA traces [Fig. 2(b)], showing that the free-running state was maintained for the whole period of observation.

Figure 2(c) depicts the output power fluctuations at the Drop port, which were always below $\pm 0.5\%$ of the average power (16 mW). Within this period of observation, the repetition rate drifted by approximately 20 kHz over an absolute frequency of approximately 48.894 GHz [Fig. 2(d)], while the carrier frequency drifted by approximately 50 MHz over an absolute frequency of approximately 194.2 THz [Fig. 2(e)]. A better understanding of the stability of the microcomb can be obtained by looking at the Allan deviations [Fig. 2(f)] evaluated for the temporal series [Figs. 2(d) and 2(e)].

If we consider the Allan deviation for the carrier frequency at 1 s gate time, we get a value of 3.55×10^{-10} , which is of the same order

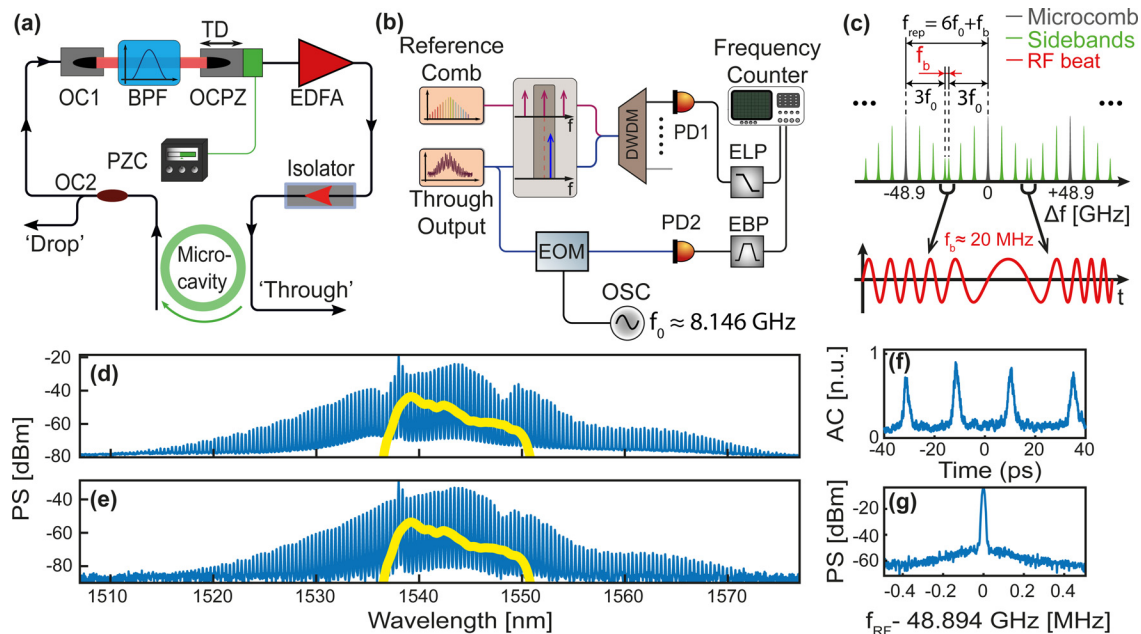


FIG. 1. Experimental setup, measurement techniques, and typical soliton state. (a) A micro-ring cavity (green) is nested into a fiber-loop featuring an erbium-doped fiber amplifier (EDFA), a bandpass filter (BPF), and free-space optical couplers (OC1, OCPZ). The OCPZ is mechanically coupled to a piezo actuator driven by a piezo controller (PZC). An optical coupler (OC2) extracts the Drop output. (b) The through output is split into two arms. One is interfered with a reference comb and is filtered with a DWDM to extract the frequency portion relative to the carrier comb line. The optical signal is then revealed with a photodiode (PD1), electrically low-pass filtered (ELP), and subsequently frequency-counted. The signal in the second arm is sent to the electro-optical modulator (EOM) driven by a GPS-referenced microwave oscillator (OSC) at $f_0 \approx 8.146$ GHz. The modulated signal is revealed with a PD (PD2) and is bandpass filtered (EBP) to improve the Signal to Noise Ratio (SNR) and frequency counted. (c) Repetition rate extraction technique. The EOM is driven by a strong microwave signal in its saturation region. The sidebands corresponding to the third harmonics of the microwave signal contribute to an RF beat-note ($f_b \approx 20$ MHz) accessible after photo-detection. (d) and (e) optical spectrum analyzer (OSA) power spectrum (PS) traces at the Through (d) and Drop (e) ports with the gain profile of the system superimposed in yellow. The gain profile accounts for both the EDFA and the intracavity BPF properties. (f) Normalized auto-correlator (AC) trace of the Drop output. (g) electrical spectrum analyzer (ESA) power spectrum (PS) trace of the down-converted repetition rate signal (resolution bandwidth, 10 kHz; video bandwidth, 1 kHz).

of magnitude as the free-running performance of a state-of-the-art fiber laser (e.g., about 5×10^{-10} in Ref. 54).

These results are, therefore, compatible with the performance expected from a free-running, mode-locked fiber comb. Figure 2(f) shows that the minimum Allan deviation is 4.35×10^{-11} for the carrier frequency, and 1.05×10^{-9} for the repetition rate, and both were obtained at the same averaging time of 64 ms. Regarding the results on the repetition rate, in particular, we obtained 4.95×10^{-9} at 1 s gate time, which is in line with the state-of-the-art results for microcombs,^{21–24,27} summarized in the introduction. The short-term stability is also evident from the good phase noise properties of the down-converted repetition rate signal [Fig. 2(g)]. Our technique did not generally allow a broadband evaluation because we necessarily had to filter the spurious frequency harmonics resulting from the modulation, and our ESA (HAMEG HMS-X) limited the acquisition. Specifically, our ESA had an intrinsic phase noise above -85 dBc/Hz at 20 kHz offset. Figure 2(g) shows a phase noise of approximately -83 dBc/Hz at 22 kHz offset. While better values have been reported in the literature (e.g., -120 dBc/Hz at 20 kHz, see Ref. 21, but also in Ref. 29), our measurement indicates that we reached the noise limit of our technique.

In assessing the stability of the system, it is essential to recall the physics sustaining these soliton states in our nested-cavity configuration, where the soliton states behave as the dominant attractors. As discussed in Ref. 44, the self-emerging solitons result from balancing

the thermal and gain nonlinearities of the system. Such nonlinearities induce a natural self-locking of the microcomb laser lines on the red-detuned slope of the microcavity resonances. This red-detuned configuration is necessary to enable stable solitary operation. We expect the stability of the carrier frequency to be dominated by the microcavity drifts: a frequency variation of 50 MHz implies a shift of the microcavity resonance, with the main cavity modes locked to the microcavity resonance red-detuned slopes. The microcavity has a linewidth of ~ 150 MHz, and solitons are observed in a red-detuned position between 40 and 50 MHz from the center. The variation in the repetition rate, conversely, depends on the stability of the fiber cavity length, generally affecting the group velocity of the pulses.

The slow nonlinearities of the system that maintain the state operate on time scales of tenths of milliseconds for the microcavity thermal detuning and tens of milliseconds for the gain response of the fiber cavity. Hence, these effects act below the gate time showing the minimum Allan deviations. Above few tens of milliseconds, the system experiences the general environmental instabilities expected from a fiber laser, although it remarkably operates at a very pure high harmonic of the repetition rate [Fig. 2(g)].

Further insight into the behavior of the system can be obtained by studying its response to the modulation of two easily accessible degrees of freedom of our system, namely the pump current of the EDFA and the main cavity length. The former was modulated by

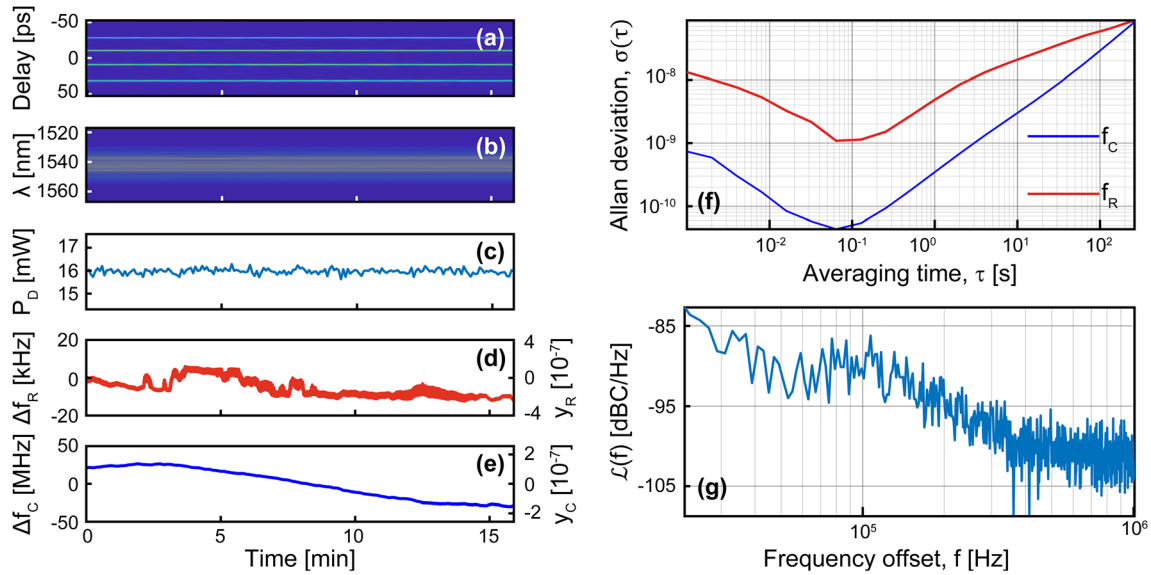


FIG. 2. Free running characterization and frequency stability analysis. The system stability is assessed for approximately 15 min. (a) Continuous acquisition of AC traces at the Drop port. (b) Continuous acquisition of OSA traces at the Drop port. (c) On-chip drop power. (d) Frequency variations of the repetition rate Δf_R (left axis) with fractional stability y_R (right axis). (e) Frequency variations of the carrier frequency Δf_C with fractional stability y_C (right axis). Reference repetition-rate frequency: 48.893 941 GHz. (f) Fractional Allan deviation $\sigma(\tau)$ of the carrier frequency (f_C) and repetition rate (f_R). Gate time of 1 ms. (g) Single sideband phase noise $\mathcal{L}(f)$ of the down-converted repetition rate RF signal. Sweep-time 100 ms. We obtain a phase noise of approximately -83 dBc/Hz at 22 kHz offset, indicating that we reach the phase noise limit of our instrument.

injecting a sinusoidal voltage waveform at the control input of the pump driver. The modulation amplitude was set to 6 mA, about 0.5% of the static pump current, which was set to 1.320 A. The cavity length, conversely, was modulated by injecting a sinusoidal waveform at the input of the piezo controller. The mechanical amplitude of the piezo oscillations was set to $0.3 \mu\text{m}$, while we estimated the effective free-space equivalent main cavity length to be approximately 3.1 m, hence, corresponding to a fractional variation of 10^{-7} . We modulated the two degrees of freedom independently on the same solitary state (Fig. 3). We can clearly see the frequency quantities responding at the imposed

control frequency for each of the modulations imposed. The close-ups in Fig. 3 further confirm that, and the OSA traces highlight that the state is preserved throughout the control experiment. We then collected the amplitude of the fractional variations for every modulation frequency, degree of freedom, and frequency quantity of interest. These results are summarized in Fig. 4. In particular, the variations of the main cavity length affect both the carrier and the repetition rate, almost constantly within the frequency span used here and within the same order of magnitude. A variation of about 10^{-7} of the cavity length produces a comparable fractional change (1×10^{-8} for F_{CL} and 2×10^{-8} for F_{RL})

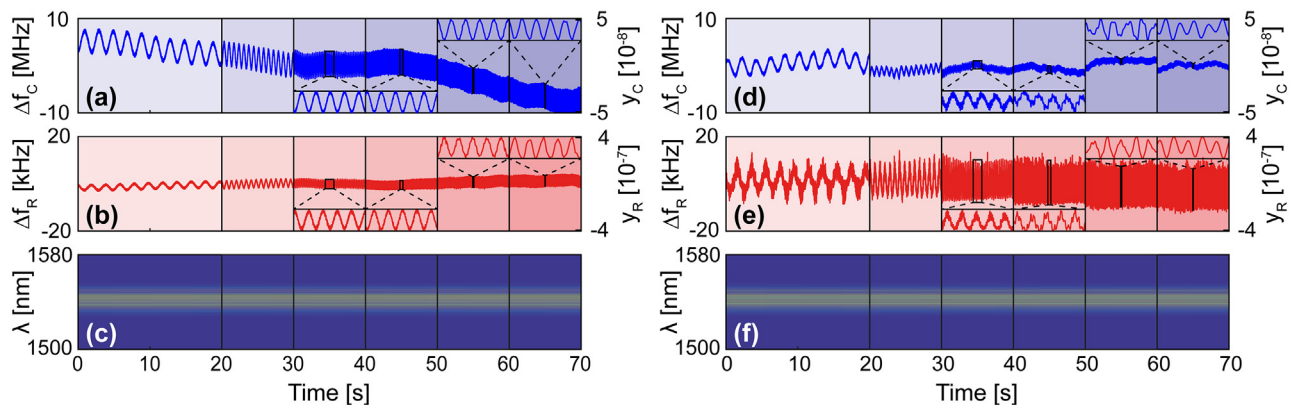


FIG. 3. Individual modulation of the main cavity length (a)–(c) and pump current (d)–(f) degrees of freedom. The control frequency was swept to cover an equidistant logarithmic span of six points from 0.5 to 100 Hz (0.5, 1.44, 4.16, 12.01, 34.65, 100 Hz). The darker background color in the frequency traces highlights the change to a higher control frequency. Each modulation frequency is applied for 10 s, except for the first one (0.5 Hz), which is applied for 20 s to record several complete cycles. The insets corresponding to the last four control frequencies provide each trace with a zoom of five control frequency cycles: (a) and (d) the carrier frequency variations (left axes) with fractional stabilities (right axes); (b) and (e) the repetition rate frequency variations (left axes) with fractional stabilities (right axes); (c) and (f) the continuously acquired OSA traces at the Drop port.

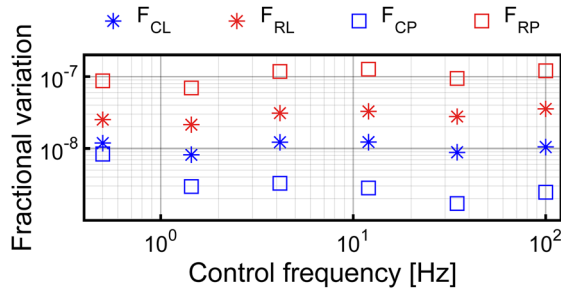


FIG. 4. Fractional variations of carrier and repetition rate. F_{CL} (F_{CP}) is the fractional variation of the carrier when the cavity length (pump current) is modulated, whereas F_{RL} (F_{RP}) is the relative variation of the repetition rate when the cavity length (pump current) is modulated.

on both the carrier and the repetition rate, respectively (see Fig. 4). Such a feature confirms that the cavity length dominates the position of the lasing modes and their mutual distances, as the soliton states are sustained by a single leading “supermode” filtered by the microcavity resonances. Conversely, the modulation of the pump current does not act the same way on the two quantities as it affects the phase and the group indices within the EDFA differently. It has a strong effect on the repetition rate, inducing an almost constant variation of 1×10^{-7} in the span of frequencies explored (see Fig. 4, F_{RP}). Differently, the effect on the carrier frequency drops dramatically even after only a few Hz (see Fig. 4, F_{CP}), in agreement with the frequency at which the Allan deviation reaches its minimum [$1 \div 64 \text{ ms} \approx 16 \text{ Hz}$, see Fig. 2(f)].

In conclusion, we have demonstrated that laser cavity-soliton combs are a stable and powerful optical source. For the repetition rate frequency, we found an Allan deviation at 1 s gate time of 4.95×10^{-9} , while for the carrier frequency, we measured a value of 3.55×10^{-10} . These values compare very well with the state-of-the-art in fiber and microcomb sources. We have identified two easily accessible degrees of freedom to control the carrier and the repetition rate frequency (i.e., the cavity length and the pump current). The remarkable free-running stability of these two quantities and the identification of two independent control parameters pave the way for locking the frequency of these sources to standard metrological references.

This study was supported by grants from EPSRC UKRI (EP/S001018/1), UK Canada Quantum Technology Programme Innovate UK (77087), ERC (851758 TELSCOMBE), DSTL (DSTLX1000142078), Leverhulme Trust (ECF-2020-537 and ECF-2022-710), ERC (TIMING 725046), NSERC (Strategic, and Discovery Grants Schemes), Canada Research Chair, and MESI PSR-SIIRI Initiatives in Quebec. We thank Dr. Reuben Harding for enlightening discussions.

AUTHOR DECLARATIONS

Conflict of Interest

The authors have no conflicts to disclose.

Author Contributions

Antonio Cutrona: Investigation (lead); Methodology (lead); Software (equal); Writing – original draft (lead); Writing – review & editing

(equal). **Maxwell Rowley:** Methodology (supporting); Software (equal); Writing – review & editing (equal). **Abdelkrim Bendahmane:** Investigation (equal); Methodology (equal); Supervision (equal). **Vittorio Ceconi:** Methodology (supporting); Writing – review & editing (equal). **Luke Peters:** Writing – review & editing (equal). **Luana Olivieri:** Writing – review & editing (equal). **Brent Little:** Resources (equal); Writing – review & editing (equal). **Sai Tak Chu:** Resources (equal); Writing – review & editing (equal). **Salvatore Stivala:** Writing – review & editing (equal). **Roberto Morandotti:** Writing – review & editing (equal). **David James Moss:** Writing – review & editing (equal). **Juan Sebastian Toter Gongora:** Funding acquisition (equal); Supervision (equal); Validation (equal); Writing – review & editing (equal). **Marco Peccianti:** Funding acquisition (equal); Methodology (equal); Project administration (equal); Supervision (equal); Validation (equal); Writing – review & editing (equal). **Alessia Pasquazi:** Funding acquisition (lead); Methodology (equal); Project administration (lead); Supervision (lead); Validation (lead); Writing – review & editing (lead).

DATA AVAILABILITY

The data that support the findings of this study are available from the corresponding authors upon reasonable request.

REFERENCES

- L. A. Lugiato, F. Prati, and M. Brambilla, *Nonlinear Optical Systems* (Cambridge University Press, 2015).
- S. Barland, S. Coen, M. Erkintalo, M. Giudici, J. Javaloyes, and S. Murdoch, “Temporal localized structures in optical resonators,” *Adv. Phys.: X* **2**(3), 496–517 (2017).
- T. J. Kippenberg, R. Holzwarth, and S. A. Diddams, “Microresonator-based optical frequency combs,” *Science* **332**(6029), 555–559 (2011).
- A. Pasquazi, M. Peccianti, L. Razzari, D. J. Moss, S. Coen, M. Erkintalo, Y. K. Chembo, T. Hansson, S. Wabnitz, P. Del’Haye, X. Xue, A. M. Weiner, and R. Morandotti, “Micro-combs: A novel generation of optical sources,” *Phys. Rep.* **729**, 1–81 (2018).
- F. Leo, S. Coen, P. Kockaert, S.-P. Gorza, P. Emplit, and M. Haelterman, “Temporal cavity solitons in one-dimensional Kerr media as bits in an all-optical buffer,” *Nat. Photonics* **4**(7), 471–476 (2010).
- T. Herr, V. Brasch, J. D. Jost, C. Y. Wang, N. M. Kondratiev, M. L. Gorodetsky, and T. J. Kippenberg, “Temporal solitons in optical microresonators,” *Nat. Photonics* **8**(2), 145–152 (2013).
- P. Marin-Palomó, J. N. Kemal, M. Karpov, A. Kordts, J. Pfeifle, M. H. P. Pfeiffer, P. Trocha, S. Wolf, V. Brasch, M. H. Anderson, R. Rosenberger, K. Vijayan, W. Freude, T. J. Kippenberg, and C. Koos, “Microresonator-based solitons for massively parallel coherent optical communications,” *Nature* **546**(7657), 274–279 (2017).
- M.-G. Suh and K. J. Vahala, “Soliton microcomb range measurement,” *Science* **359**(6378), 884–887 (2018).
- B. Corcoran, M. Tan, X. Xu, A. Boes, J. Wu, T. G. Nguyen, S. T. Chu, B. E. Little, R. Morandotti, A. Mitchell, and D. J. Moss, “Ultra-dense optical data transmission over standard fibre with a single chip source,” *Nat. Commun.* **11**(1), 2568 (2020).
- J. Liu, H. Tian, E. Lucas, A. S. Raja, G. Lihachev, R. N. Wang, J. He, T. Liu, M. H. Anderson, W. Weng, S. A. Bhave, and T. J. Kippenberg, “Monolithic piezoelectric control of soliton microcombs,” *Nature* **583**(7816), 385–390 (2020).
- X. Xu, M. Tan, B. Corcoran, J. Wu, A. Boes, T. G. Nguyen, S. T. Chu, B. E. Little, D. G. Hicks, R. Morandotti, A. Mitchell, and D. J. Moss, “11 TOPS photonic convolutional accelerator for optical neural networks,” *Nature* **589**(7840), 44–51 (2021).
- A. Dutt, C. Joshi, X. Ji, J. Cardenas, Y. Okawachi, K. Luke, A. L. Gaeta, and M. Lipson, “On-chip dual-comb source for spectroscopy,” *Sci. Adv.* **4**(3), e1701858 (2018).

- ¹³B. Stern, X. Ji, Y. Okawachi, A. L. Gaeta, and M. Lipson, "Battery-operated integrated frequency comb generator," *Nature* **562**(7727), 401–405 (2018).
- ¹⁴J. Riemensberger, A. Lukashchuk, M. Karpov, W. Weng, E. Lucas, J. Liu, and T. J. Kippenberg, "Massively parallel coherent laser ranging using a soliton microcomb," *Nature* **581**(7807), 164–170 (2020).
- ¹⁵W. Liang, D. Eliyahu, V. S. Ilchenko, A. A. Savchenkov, A. B. Matsko, D. Seidel, and L. Maleki, "High spectral purity Kerr frequency comb radio frequency photonic oscillator," *Nat. Commun.* **6**(1), 7957 (2015).
- ¹⁶Y. K. Chembo, "Kerr optical frequency combs: Theory, applications and perspectives," *Nanophotonics* **5**(2), 214–230 (2016).
- ¹⁷N. Picqué and T. W. Hänsch, "Frequency comb spectroscopy," *Nat. Photonics* **13**(3), 146–157 (2019).
- ¹⁸L. Lugiato, F. Prati, and M. Brambilla, *Nonlinear Optical Systems* (Cambridge University Press, 2015).
- ¹⁹J. M. C. Boggio, D. Bodenmüller, S. Ahmed, S. Wabnitz, D. Modotto, and T. Hansson, "Efficient Kerr soliton comb generation in micro-resonator with interferometric back-coupling," *Nat. Commun.* **13**(1), 1292 (2022).
- ²⁰P. Del'Haye, S. B. Papp, and S. A. Diddams, "Hybrid electro-optically modulated microcombs," *Phys. Rev. Lett.* **109**(26), 263901 (2012).
- ²¹J. Liu, E. Lucas, A. S. Raja, J. He, J. Riemensberger, R. N. Wang, M. Karpov, H. Guo, R. Bouchand, and T. J. Kippenberg, "Photonic microwave generation in the X- and K-band using integrated soliton microcombs," *Nat. Photonics* **14**(8), 486–491 (2020).
- ²²T. Tetsumoto, J. Jiang, M. E. Fermann, G. Navickaite, M. Geiselmann, and A. Rolland, "Effects of a quiet point on a Kerr microresonator frequency comb," *OSA Continuum* **4**(4), 1348 (2021).
- ²³S. Zhang, J. M. Silver, X. Shang, L. Del Bino, N. M. Ridler, and P. Del'Haye, "Terahertz wave generation using a soliton microcomb," *Opt. Express* **27**(24), 35257 (2019).
- ²⁴A. K. Vinod, S.-W. Huang, J. Yang, M. Yu, D.-L. Kwong, and C. W. Wong, "Frequency microcomb stabilization via dual-microwave control," *Commun. Phys.* **4**(1), 81 (2021).
- ²⁵S. Zhang, J. M. Silver, L. Del Bino, F. Copie, M. T. M. Woodley, G. N. Ghalanos, A. Ø. Svela, N. Moroney, and P. Del'Haye, "Sub-milliwatt-level microresonator solitons with extended access range using an auxiliary laser," *Optica* **6**(2), 206–212 (2019).
- ²⁶H. Weng, A. A. Afridi, J. Li, M. McDermott, H. Tu, L. P. Barry, Q. Lu, W. Guo, and J. F. Donegan, "Dual-mode microresonators as straightforward access to octave-spanning dissipative Kerr solitons," *APL Photonics* **7**(6), 066103 (2022).
- ²⁷Y. Bai, M. Zhang, Q. Shi, S. Ding, Y. Qin, Z. Xie, X. Jiang, and M. Xiao, "Briouin-Kerr soliton frequency combs in an optical microresonator," *Phys. Rev. Lett.* **126**(6), 063901 (2021).
- ²⁸F. Lei, Z. Ye, Ö. B. Helgason, A. Fülöp, M. Girardi, and V. Torres-Company, "Optical linewidth of soliton microcombs," *Nat. Commun.* **13**(1), 3161 (2022).
- ²⁹M. Nie, K. Jia, J. Bartos, S. Zhu, Z. Xie, and S.-W. Huang, "Turnkey photonic flywheel in a Chimera cavity," *arXiv:2212.14120* (2022).
- ³⁰W. Jin, Q.-F. Yang, L. Chang, B. Shen, H. Wang, M. A. Leal, L. Wu, M. Gao, A. Feshali, M. Paniccia, K. J. Vahala, and J. E. Bowers, "Hertz-line-width semiconductor lasers using CMOS-ready ultra-high-Q microresonators," *Nat. Photonics* **15**, 346–353 (2021).
- ³¹K. Volyanskiy, P. Salzenstein, H. Tavernier, M. Pogurmirskiy, Y. K. Chembo, and L. Larger, "Compact optoelectronic microwave oscillators using ultra-high Q whispering gallery mode disk-resonators and phase modulation," *Opt. Express* **18**(21), 22358–22363 (2010).
- ³²A. A. Savchenkov, D. Eliyahu, W. Liang, V. S. Ilchenko, J. Byrd, A. B. Matsko, D. Seidel, and L. Maleki, "Stabilization of a Kerr frequency comb oscillator," *Opt. Lett.* **38**(15), 2636–2639 (2013).
- ³³S. B. Papp, K. Beha, P. Del'Haye, F. Quinlan, H. Lee, K. J. Vahala, S. A. Diddams, P. Del'Haye, F. Quinlan, H. Lee, K. J. Vahala, and S. A. Diddams, "Microresonator frequency comb optical clock," *Optica* **1**(1), 10–14 (2014).
- ³⁴P. Del'Haye, A. Coillet, T. Fortier, K. Beha, D. C. Cole, K. Y. Yang, H. Lee, K. J. Vahala, S. B. Papp, and S. A. Diddams, "Phase-coherent microwave-to-optical link with a self-referenced microcomb," *Nat. Photonics* **10**(8), 516–520 (2016).
- ³⁵V. Brasch, E. Lucas, J. D. Jost, M. Geiselmann, and T. J. Kippenberg, "Self-referenced photonic chip soliton Kerr frequency comb," *Light: Sci. Appl.* **6**(1), e16202 (2017).
- ³⁶L. Stern, J. R. Stone, S. Kang, D. C. Cole, M.-G. Suh, C. Fredrick, Z. Newman, K. Vahala, J. Kitching, S. A. Diddams, and S. B. Papp, "Direct Kerr frequency comb atomic spectroscopy and stabilization," *Sci. Adv.* **6**(9), eaax6230 (2020).
- ³⁷D. T. Spencer, T. Drake, T. C. Briles, J. Stone, L. C. Sinclair, C. Fredrick, Q. Li, D. Westly, B. R. Ilic, A. Bluestone, N. Volet, T. Komljenovic, L. Chang, S. H. Lee, D. Y. Oh, M.-G. Suh, K. Y. Yang, M. H. P. Pfeiffer, T. J. Kippenberg, E. Norberg, L. Theogarajan, K. Vahala, N. R. Newbury, K. Srinivasan, J. E. Bowers, S. A. Diddams, and S. B. Papp, "An optical-frequency synthesizer using integrated photonics," *Nature* **557**(7703), 81–88 (2018).
- ³⁸B. Li, W. Jin, L. Wu, L. Chang, H. Wang, B. Shen, Z. Yuan, A. Feshali, M. Paniccia, K. J. Vahala, and J. E. Bowers, "Reaching fiber-laser coherence in integrated photonics," *Opt. Lett.* **46**(20), 5201 (2021).
- ³⁹L. Stern, W. Zhang, L. Chang, J. Guo, C. Xiang, M. A. Tran, D. Huang, J. D. Peters, D. Kinghorn, J. E. Bowers, and S. B. Papp, "Ultra-precise optical-frequency stabilization with heterogeneous III-V/Si lasers," *Opt. Lett.* **45**(18), 5275 (2020).
- ⁴⁰M. Peccianti, A. Pasquazi, Y. Park, B. E. Little, S. T. Chu, D. J. Moss, and R. Morandotti, "Demonstration of a stable ultrafast laser based on a nonlinear microcavity," *Nat. Commun.* **3**, 765 (2012).
- ⁴¹A. Pasquazi, M. Peccianti, B. E. Little, S. T. Chu, D. J. Moss, and R. Morandotti, "Stable, dual mode, high repetition rate mode-locked laser based on a microring resonator," *Opt. Express* **20**(24), 27355–27362 (2012).
- ⁴²H. Bao, A. Cooper, M. Rowley, L. Di Lauro, J. S. Toterogongora, S. T. Chu, B. E. Little, G.-L. Oppo, R. Morandotti, D. J. Moss, B. Wetzell, M. Peccianti, and A. Pasquazi, "Laser cavity-soliton microcombs," *Nat. Photonics* **13**(6), 384–389 (2019).
- ⁴³A. Cutrona, P.-H. Hanzard, M. Rowley, J. S. Toterogongora, M. Peccianti, B. A. Malomed, G.-L. Oppo, and A. Pasquazi, "Temporal cavity solitons in a laser-based microcomb: A path to a self-starting pulsed laser without saturable absorption," *Opt. Express* **29**(5), 6629–6646 (2021).
- ⁴⁴M. Rowley, P.-H. Hanzard, A. Cutrona, H. Bao, S. T. Chu, B. E. Little, R. Morandotti, D. J. Moss, G.-L. Oppo, J. S. Toterogongora, M. Peccianti, and A. Pasquazi, "Self-emergence of robust solitons in a microcavity," *Nature* **608**(7922), 303–309 (2022).
- ⁴⁵A. Cutrona, A. Cutrona, M. Rowley, D. Das, D. Das, L. Olivieri, L. Olivieri, L. Peters, L. Peters, S. T. Chu, B. E. Little, R. Morandotti, D. J. Moss, J. S. T. Gongora, J. S. T. Gongora, M. Peccianti, M. Peccianti, A. Pasquazi, and A. Pasquazi, "High parametric efficiency in laser cavity-soliton microcombs," *Opt. Express* **30**(22), 39816–39825 (2022).
- ⁴⁶C. Lecaplain and P. Grelu, "Multi-gigahertz repetition-rate-selectable passive harmonic mode locking of a fiber laser," *Opt. Express* **21**(9), 10897 (2013).
- ⁴⁷C. S. Jun, J. H. Im, S. H. Yoo, S. Y. Choi, F. Rotermund, D.-I. Yeom, and B. Y. Kim, "Low noise GHz passive harmonic mode-locking of soliton fiber laser using evanescent wave interaction with carbon nanotubes," *Opt. Express* **19**(20), 19775 (2011).
- ⁴⁸A. B. Grudinin, D. J. Richardson, and D. N. Payne, "Passive harmonic mode-locking of a fibre soliton ring laser," *Electron. Lett.* **29**(21), 1860–1861 (1993).
- ⁴⁹Z. Wang, L. Zhan, A. Majeed, and Z. Zou, "Harmonic mode locking of bound solitons," *Opt. Lett.* **40**(6), 1065–1068 (2015).
- ⁵⁰F. Amrani, F. Haboucha, M. Sallhi, H. Leblond, A. Komarov, P. Grelu, and F. Sanchez, "Passively mode-locked erbium-doped double-clad fiber laser operating at the 322nd harmonic," *Opt. Lett.* **34**(14), 2120 (2009).
- ⁵¹A. B. Grudinin, D. J. Richardson, and D. N. Payne, "Energy quantisation in figure eight fibre laser," *Electron. Lett.* **28**(1), 67–68 (1992).
- ⁵²J. Schröder, D. Alasia, T. Sylvestre, and S. Coen, "Dynamics of an ultrahigh-repetition-rate passively mode-locked Raman fiber laser," *J. Opt. Soc. Am. B* **25**(7), 1178 (2008).
- ⁵³R. Si Fodil, F. Amrani, C. Yang, A. Kellou, and P. Grelu, "Adjustable high-repetition-rate pulse trains in a passively-mode-locked fiber laser," *Phys. Rev. A* **94**(1), 013813 (2016).
- ⁵⁴H. Tian, F. Meng, K. Wang, B. Lin, S. Cao, Z. Fang, Y. Song, and M. Hu, "Optical frequency comb stabilized to a fiber delay line," *Appl. Phys. Lett.* **119**(12), 121106 (2021).
- ⁵⁵T. R. Schibli, K. Minoshima, F.-L. Hong, H. Inaba, A. Onae, H. Matsumoto, I. Hartl, and M. E. Fermann, "Frequency metrology with a turnkey all-fiber system," *Opt. Lett.* **29**(21), 2467–2469 (2004).

- ⁵⁶V. Ribeiro, A. D. Szabo, A. M. Rocha, C. B. Gaur, A. A. I. Ali, Y. Quiquempois, A. Mussot, G. Bouwmans, and N. Doran, "Parametric amplification and wavelength conversion in dual-core highly nonlinear fibers," *J. Lightwave Technol.* **40**(17), 6013–6020 (2022).
- ⁵⁷A. Mussot, C. Naveau, M. Conforti, A. Kudlinski, F. Copie, P. Szriftgiser, and S. Trillo, "Fibre multi-wave mixing combs reveal the broken symmetry of Fermi–Pasta–Ulam recurrence," *Nat. Photonics* **12**(5), 303–308 (2018).
- ⁵⁸N. Englebert, F. De Lucia, P. Parra-Rivas, C. M. Arabi, P.-J. Sazio, S.-P. Gorza, and F. Leo, "Parametrically driven Kerr cavity solitons," *Nat. Photonics* **15**(11), 857–861 (2021).
- ⁵⁹M. Leonhardt, D. Paligora, N. Englebert, F. Leo, J. Fatome, and M. Erkintalo, "Parametrically-driven temporal cavity solitons in a bichromatically-driven pure Kerr resonator," [arXiv:2206.09533](https://arxiv.org/abs/2206.09533) (2022).
- ⁶⁰E. J. Tough, M. J. Fice, C. C. Renaud, J. Seddon, A. J. Seeds, C. Graham, K. Balakier, and G. Carpintero, "InP photonic integrated circuit for 6.7GHz spaced optical frequency comb generator," in *International Topical Meeting on Microwave Photonics (MWP)* (IEEE, 2021).
- ⁶¹A. Rolland, G. Loas, M. Brunel, L. Frein, M. Vallet, and M. Alouini, "Non-linear optoelectronic phase-locked loop for stabilization of opto-millimeter waves: Towards a narrow linewidth tunable THz source," *Opt. Express* **19**(19), 17944 (2011).